J. Am. Chem. Soc. **1996,** *118,* 5254−5260

Can Fulvene S_1 Decay Be Controlled? A CASSCF Study with MMVB Dynamics

Michael J. Bearpark,[†] Fernando Bernardi,[‡] Massimo Olivucci,*,[‡] Michael A. Robb,*,[†] and Barry R. Smith[†]

Contribution from the Dipartimento di Chimica "G. Ciamician" dell' Università di Bologna, Via Selmi 2, 40126 Bologna, Italy, and Department of Chemistry, King's College London, Strand, London WC2R 2LS, U.K.

Received December 22, 1995. Revised Manuscript Received April 1, 1996[⊗]

Abstract: CASSCF and CASMP2 calculations show that the minimum on the fulvene S_1 potential energy surface is an S_0/S_1 conical intersection with a 90° twisted methylene group. We have also located a distinct planar azulene-like crossing point at higher energy, where the methylene is free to twist. The fulvene intersection—which exists for all twist angles—leads to efficient, irreversible radiationless decay and explains the lack of observed S_1 fluorescence. We have modeled the femtosecond excited state motion leading to ultrafast decay that would be initiated by exciting the 0−0 and higher vibrational levels using semiclassical molecular dynamics with a hybrid quantum-mechanical/force-field potential (MMVB). Our simulation suggests that, with increased vibrational energy, decay occurs in the planar crossing region before relaxation by twisting can take place, and that isomerization might only be seen by pumping the 0−0 transition in laser studies.

Introduction

Beer and Longuet-Higgins[1] found that the S_1 state of azulene was nonfluorescent, and suggested that this was due to fast nonradiative decay at a real crossing (conical intersection[2]) of the S_1 and S_0 potential energy surfaces. We have recently characterized such a crossing at the CASSCF/6-31G* level of theory[3] and modeled the radiationless decay dynamics semiclassically using the method described in ref 4. In this paper, we show that the nonfluorescent S_1 state of fulvene can decay at a planar azulene-like S_0/S_1 conical intersection even though the lowest-energy point on the intersection—the minimum on S_1 overall—is 90° twisted.

Figure 1 (top) illustrates azulene relaxation from the Franck−Condon geometry (S_0^*) on S_1, which takes place in a deep well leading to a planar S_0/S_1 crossing (dashed line) a few kilocalories per mole above the minimum. Our semiclassical dynamics

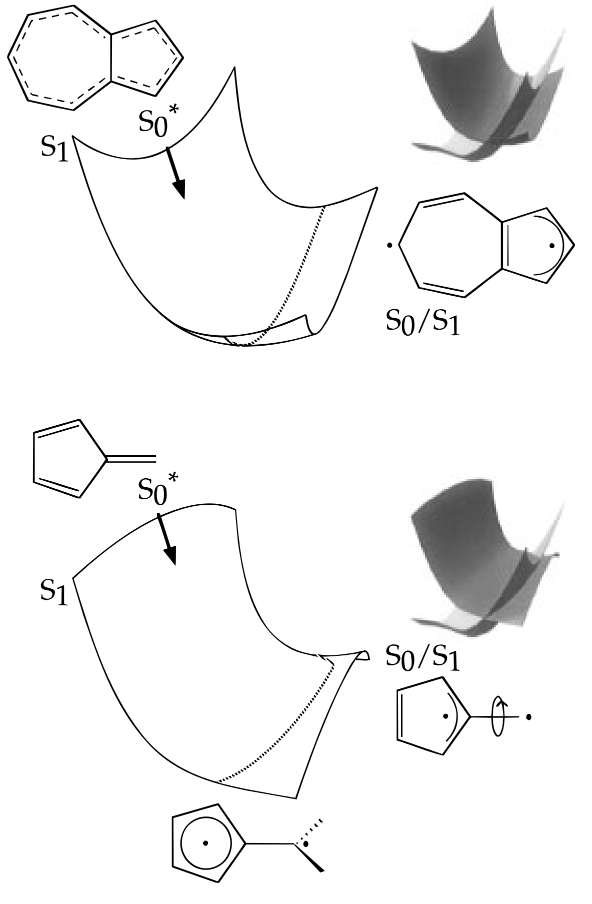

Figure 1. A schematic representation of the S_1 potential energy surfaces of azulene (top) and fulvene (bottom). The S_0/S_1 conical intersections are represented by a dashed line. The planar fulvene crossing is a local maximum with respect to twisting of the methylene group. The *x* coordinate (left to right in the figure) refers to the "localization" coordinate of the 5-membered ring that corresponds mainly to the trans annular bond in azulene. The *z* coordinate (coming out of the plane of the page) corresponds to ring deformation in azulene and methyl twisting in fulvene.

[†] King's College London.

[‡] Università di Bologna.

[⊗] Abstract published in *Advance ACS Abstracts,* May 15, 1996.

(1) Beer, M.; Longuet-Higgins, H. C. *J. Chem. Phys.* **1955**, *23*, 1390−1391.

(2) (a) A conical intersection is an $n - 2$ dimensional subspace of n nuclear coordinates in which two states are degenerate. Movement along the 2 remaining linearly-independent nuclear coordinates (the nonadiabatic coupling and gradient difference vectors) lifts the degeneracy. (b) Teller, E. *J. Phys. Chem.* **1937**, *41*, 109. (c) Kauzmann, W. *Quantum Chemistry*; Academic Press: New York, 1957; pp 696−697. (e) Herzberg, G.; Longuett-Higgins, H. C. *Discuss. Faraday Soc.* **1963**, *35*, 77. (f) Herzberg, G. *The Electronic Spectra of Polyatomic Molecules*; Van Nostrand: Princeton, 1966, p 442. (g) Teller, E. *Isr. J. Chem.* **1969**, *7*, 227−235. (h) Longuet-Higgins, H. C. *Proc. R. Soc. London A* **1975**, *344*, 147−156. (i) Gerhartz, W.; Poshusta, R. D.; Michl, J. *J. Am. Chem. Soc.* **1977**, *99*, 4263. (j) Salem, L. *Electrons in Chemical Reactions: First Principles*; Wiley: New York, 1982; pp 148−153. (k) Bonacic-Koutecky, V.; Koutecky, J.; Michl, J. *Angew. Chem., Int. Ed. Engl.* **1987**, *26*, 170−189. (l) Michl, J.; Bonacic-Koutecky, V. *Tetrahedron* **1988**, *44*, 7559. (m) Michl, J.; Bonacic-Koutecky, V. *Electronic Aspects of Organic Photochemistry*; Wiley: New York, 1990; p 66. (n) Keating, S. P.; Mead, C. A. *J. Chem. Phys.* **1987**, *86*, 2152. (o) Blais, N. C.; Truhlar, D. G.; Mead, C. A. *J. Chem. Phys.* **1988**, *89*, 6204. (p) Manthe, U.; Koppel, H. *J. Chem. Phys.* **1990**, *93*, 1658. (q) Xantheas, S. S.; Ruedenberg, K. *J. Chem. Phys.* **1991**, *95*, 1862.

(3) Bearpark, M. J.; Bernardi, F.; Clifford, S.; Olivucci, M.; Robb, M. A.; Smith, B. R.; Vreven, T. *J. Am. Chem. Soc.* **1996**, *118*, 169−175.

(4) Smith, B. R.; Bearpark, M. J.; Robb, M. A.; Bernardi, F.; Olivucci, M. *Chem. Phys. Lett.* **1995**, *242*, 27−32.

S0002-7863(95)04279-X CCC: $12.00

simulation[3,4] suggests that azulene $S_1 \rightarrow S_0$ decay takes place in femtoseconds before a single oscillation in the S_1 well is completed. In contrast, S_1 fulvene (Figure 1, bottom) has a double well potential. The global minima are 90° twisted points on an S_0/S_1 crossing which persists for all twist angles, including a planar azulene-like critical point which is unstable toward methylene twisting. In simulating the 0−0 excitation of fulvene to S_1, we find that increasing the initial vibrational excess energy leads to decay in the planar crossing region before relaxation by twisting can take place.[5] *Cis*−*trans* isomerization may therefore only be detectable at very low excess energies.

Kent et al.[7,8] have characterized four bands in the fulvene absorption spectrum with maxima between 400 and 167 nm. S_3 and S_4 are Rydberg states;[7c] the first two bands correspond to dipole-allowed transitions to valence excited states of B_2 (S_1) and A_1 (S_2) symmetry. The S_1 band is broad, weak, and diffuse, with the 0−0 transition at 508 nm and a maximum at ∼350 nm (3.44 eV). The low oscillator strength ($f = 0.008$) is thought to arise from small Franck−Condon factors caused by a large geometry change on exciting to S_1. Vibrational structure can only be resolved at the onset of absorption.[7b] No rearrangement to benzene (which occurs on excitation to S_2) is observed,[8] and the vibronic line widths and lack of fluorescence are taken to indicate fast internal conversion back to S_0 fulvene.

Several *ab initio* calculations of fulvene excited states have recently appeared,[5,10] building on previous semiempirical[11,12] and *ab initio* work.[13,14] Galasso[10] calculated vertical excitation energies and one- and two-photon transition moments for 6 valence and 27 Rydberg excited singlet states using the random phase approximation.[15] These calculations included single excitations, although configuration interaction (CI) calculations for the valence states showed that double excitations made a significant contribution.[10] This was confirmed by Negri and Zgierski,[6] who optimized the geometry of S_1 fulvene using CIS and CASSCF in a 6-31G* basis and found that CIS underestimated the reversal of bond length alternation needed to explain the vibronic structure of this transition. The S_1 minimum optimized with planar constraint was found to have two imaginary vibrational frequencies at the CASSCF/6-31G* level, one leading to twisting and another to pyramidalization[6] of the methylene group.

Dreyer and Klessinger[5] optimized the geometries of the fulvene S_1 and S_2 states, using both MNDOC-CI and CASSCF. A planar MNDOC-CI transition structure for interconversion between two pyramidal minima was located on S_1, with a barrier height of only 0.3 kcal mol^{-1}. Both Dreyer and Klessinger and Negri and Zgierski emphasize that the energy available on relaxation from the Franck−Condon geometry (S_0^*) to the relatively flat minimum is large (>20 kcal mol^{-1}). Klessinger[5] has also shown (using MNDOC-CI) that there is a 90° twisted geometry on S_1 at which a crossing with S_0 occurs, only ∼1 kcal mol^{-1} above the slightly-pyramidalized S_1 minimum. Such a crossing could explain the lack of fluorescence from S_1 fulvene, leading to irreversible decay within a single vibrational period.[2p] For a critically-heterosymmetric biradicaloid, a two-electron two-orbital model predicts a crossing of the S_0 and S_1 states.[2k−m] MNDO/3 calculations with 3×3 CI suggest that this condition may be fulfilled for some twisted derivatives of fulvene,[16] but the crossing located by Klessinger appears not to be the one predicted for a critically-heterosymmetric biradicaloid.[5]

In this paper we report that, with CASSCF optimized geometries and CASMP2 energies, the twisted S_0/S_1 crossing described by Klessinger[5] is the lowest-energy point on S_1. We have also located an azulene-like S_0/S_1 crossing point which is planar but unstable with respect to methylene twisting, and which lies approximately 10 kcal mol^{-1} above the twisted crossing minimum. Semiclassical dynamics calculations (using a 30-dimensional, parametrized quantum-mechanical/force-field potential which reproduces the structure of the CASSCF surface) suggest that, upon increasing the initial vibrational excess energy, $S_1 \rightarrow S_0$ decay is more likely to occur in the planar region of the crossing before relaxation by twisting can take place. We therefore predict that photoisomerization of the exocyclic methylene may only result from 0−0 excitation to S_1.

Computational Methods

CASSCF geometry optimizations for the ground and valence excited states of fulvene were carried out with Gaussian 94[17] using an active space of 6 electrons in the 6 valence π orbitals (CAS6). Both 4-31G and 6-31G* basis sets were used, although previous fulvene studies[5,6] had suggested that the valence excited state geometries and vertical excitation energies would be little changed by the addition of polarization or diffuse basis functions. Energies were recomputed with CASMP2/6-31G*[18] in order to partially account for the effect of dynamic electron correlation. Minima and saddle points were characterized by analytic second derivative calculations at the CASSCF/4-31G level of theory. Stationary points along the S_0/S_1 crossing line[2,19] were located using the algorithm described in ref 20 and implemented in Gaussian 94. (Further examples of this type are discussed in ref 21).

In order to test for the possible role of ionic states in fulvene internal conversion, the twisted ring$^-$ methylene$^+$ ionic structure was optimized at the RHF/STO-3G level of theory and CASSCF energies recomputed

---

(5) Dreyer, J.; Klessinger, M. *J. Chem. Phys.* **1994**, *101*, 10655−10665.

(6) Negri, F.; Zgierski, M. Z. *J. Chem. Phys.* **1995**, *102*, 5165−5173.

(7) (a) Brown, R. D.; Domaille, P. J.; Kent, J. E. *Aust. J. Chem.* **1970**, *23*, 1707−1720. (b) Domaille, P. J.; Kent, J. E.; O'Dwyer, M. F. *Chem. Phys.* **1974**, *6*, 66−75. (c) Harman, P. J.; Kent, J. E.; O'Dwyer, M. F.; Smith, M. H. *Aust. J. Chem.* **1979**, *32*, 2579−2587.

(8) Kent, J. E.; Harman, P. J.; O'Dwyer, M. F. *J. Phys. Chem.* **1981**, *85*, 2726−2730.

(9) (a) Hunt, G. R.; Ross, I. G. *J. Mol. Spectrosc.* **1962**, *9*, 50−78. (b) McCoy, E. F.; Ross, I. G. *Aust. J. Chem.* **1962**, *18*, 573−590. (c) Hunt, G. R.; McCoy, E. F.; Ross, I. G. *Aust. J. Chem.* **1962**, *18*, 591−604. (d) Hochstrasser, R. M.; Li, T. -Y. *J. Mol. Spectrosc.* **1972**, *41*, 297−301.

(10) Galasso, V. *Chem. Phys.* **1993**, *171*, 171−178.

(11) Straub, P. A.; Meuche, D.; Heilbronner, E. *Helv. Chim. Acta* **1966**, *49*, 517.

(12) (a) Ertl, P. *Monatsh. Chem.* **1991**, *122*, 1015−1018. (b) Tinland, B. *J. Mol. Struct.* **1969**, *3*, 429−432. (c) Bloor, J. E.; Gilson, B. R.; Brearly, N. *Theor. Chim. Acta* **1967**, *8*, 35−53. (d) Brown, R. D.; Burden, F. R.; Williams, G. R. *Aust. J. Chem.* **1968**, *21*, 1939−1951. (e) Buemi, G.; Zuccarello, F.; Raudino, A. *Theochem*−*J. Mol. Struct.* **1981**, *1*, 137−164. (f) Jug, K.; Neumann, F.; Malar, E. J. P. *Theochem*−*J. Mol. Struct.* **1995**, *336*, 81−84.

(13) Praud, L.; Midlie, P.; Berthier, G. *Theor. Chim. Acta* **1968**, 11, 169−173. (b) Praud, L.; Levy, B.; Millie, P.; Berthier, G. *Int. J. Quantum Chem. Symp.* **1973**, *7*, 185−191. (c) Rancurel, P.; Huron, B.; Praud, L.; Malrieu, J. P.; Berthier, G. *J. Mol. Spectrosc.* **1976**, *60*, 259−276.

(14) (a) Mukherjee, D. *Int. J. Quantum Chem.* **1974**, *8*, 247−253. (b) Swiderek, P.; Michaud, M.; Sanche, L. *J. Chem. Phys.* **1995**, *103*, 8424−8432.

(15) (a) Rowe, D. J. *Rev. Mod. Phys.* **1963**, *40*, 153. (b) Luo, Y.; Agren, H.; Koch, H.; Jorgensen, P.; Helgaker, T. *Phys. Rev. B: Condens. Matter* **1995**, *51*, 14949−14957.

(16) Takahashi, O.; Kikuchi, O. *Tetrahedron* **1990**, *46*, 3803−3812.

(17) Gaussian 94: Frisch, M. J.; Trucks, G. W.; Schlegel, H. B.; Gill, P. M. W.; Johnson, B. G.; Robb, M. A.; Cheeseman, J. R.; Keith, T. A.; Petersson, G. A.; Montgomery, J. A.; Raghavachari, K.; Al-Laham, M. A.; Zakrzewski, V. G.; Ortiz, J. V.; Foresman, J. B.; Cioslowski, J.; Stefanov, B. B.; Nanayakkara, A.; Challacombe, M.; Peng, C. Y.; Ayala, P. Y.; Chen, W.; Wong, M. W.; Andres, J. L.; Reploge, E. S.; Gomperts, R.; Martin, R. L.; Fox, D. J.; Binkley, J. S.; Defrees, D. J.; Baker, J.; Stewart, J. P.; Head-Gordon, M.; Gonzales, C.; Pople, J. A.; Gaussian, Inc.: Pittsburgh, PA, 1995.

(18) McDouall, J. J. W.; Peasley, K.; Robb, M. A. *Chem. Phys. Lett.* **1988**, *148*, 183.

(19) Klessinger, M. *Angew. Chem., Int. Ed. Engl.* **1995**, *34*, 549−551.

Scheme 1

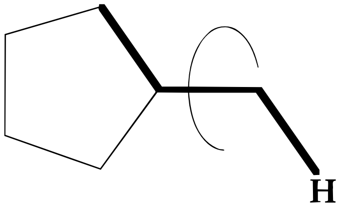

at this geometry using the 6-31+G* basis which includes polarization and diffuse functions. The RHF/STO-3G solution is ionic and provides a good guess for the S_2 state at the CASSCF level, since the S_2 CAS wave function is dominated by the SCF determinant. Because of this, the RHF/STO-3G geometry is close to the twisted S_2 minimum: reoptimizing at the 6-orbital CASSCF/6-31+G* level lowers the S_2 energy by only 5 kcal mol^{-1}. The CAS6 active space was extended by adding compact π molecular orbitals with extra nodes above and below the ring in order to account for part of the difference in dynamic electron correlation between ionic and covalent states. Further dynamic correlation was then included via CASMP2/6-31+G*.[18]

MMVB[22] —a hybrid, parametrized quantum-mechanical/force-field potential—was used to describe the valence excited states inexpensively so that all 30 nuclear degrees of freedom could be included in dynamics calculations.[4] For fulvene, MMVB correctly simulates the topology of the S_0 and S_1 CASSCF potential energy surfaces. Classical trajectories were propagated using a series of local quadratic approximations to the potential energy surface,[23] the stepsize being determined by a trust radius.[24] Initial conditions were determined by random sampling of each excited state normal mode within an energy threshold $\Delta E_{\mathrm{limit}}$. (For each value of $\Delta E_{\mathrm{limit}}$, 256 trajectories were run, each for several hundred steps.) The surface-hop algorithm of Tully and Preston[25] was used to allow excited state trajectories to hop to the ground state in the conical intersection region, where non-adiabatic coupling is strong.

Finally, in order to rationalize the electronic structure and geometries of the fulvene exited states, the MMVB eigenvectors were used to generate an "exchange" density matrix P_{ij}.[22b,26] The elements of P_{ij} have a simple physical interpretation which is related to the spin coupling between valence electrons localized in the p−π orbitals residing on the carbon atoms i and j: P_{ij} is close to +1.0 for pairs that are singlet spin coupled (bonding) and close to −1.0 for triplet (parallel, repulsive) spins (as discussed in ref 27, for example).

Results and Discussion

This section is divided into four parts. In the first, we compare the CASSCF and MMVB excitation energies at vertical and relaxed planar geometries with experiment. In the second, we describe the S_1 potential energy surface and S_0/S_1 conical intersection. In the third part, we discuss the origin of the conical intersection and show that the ionic ring$^-$ methylene$^+$ state is S_2 and well-separated energetically at this geometry. Finally, we use the results of semiclassical dynamics calculations to argue that isomerization is only likely to occur after 0−0 S_1 excitation.

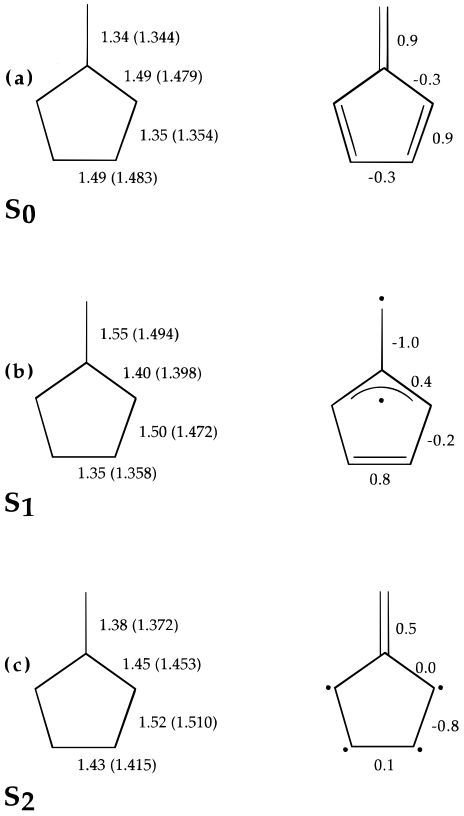

Figure 2. Optimized planar geometries **a**−**c** of the valence states of fulvene. MMVB bond lengths (Å) agree with the CASSCF/4-31G values (in parentheses) to within ±0.02 Å. The corresponding P_{ij} (π electron exchange density) values are shown on the right.

(1) Excitation Energies (Vertical and Relaxed). The methylene twist angle is measured as the dihedral shown in Scheme 1 in this paper.

Figure 2 shows that the S_0 planar optimized structure **a** consists of three double bonds with little delocalization, but that a complete inversion of single and double bond character takes place on exciting to S_1, as noted originally by Sklar.[28] This change is reflected in the spin coupling of the six π-electrons in the S_1 planar optimized structure **b**: for example, the bond to exocyclic methylene in S_0 fulvene is singlet coupled ($P_{ij} \sim$ 1.0), but becomes triplet coupled in S_1 ($P_{ij} = -1.0$) and is therefore free to twist. The S_2 planar optimized structure **c** has only one fully formed double-bond from ring to methylene, blocking the twisting motion.

The covalent nature of S_1[28] is consistent with a small $S_0 \rightarrow S_1$ transition dipole and low observed oscillator strength.[7] The large geometry change is consistent with the broad absorption spectra: because the gradient on the excited states is large at the Franck−Condon geometry, the computed vertical excitation energies will be very sensitive to the S_0 geometry used. Table 1 shows that the experimental S_1 and S_2 vertical excitation energies[7] are both overestimated at the CASSCF/4-31G level

---

(20) (a) Ragazos, I. N.; Robb, M. A.; Bernardi, F.; Olivucci, M. *Chem. Phys. Lett.* **1992**, *197*, 217. (b) Bearpark, M. J.; Robb, M. A.; Schlegel, H. B. *Chem. Phys. Lett.* **1994**, *223*, 269−274.

(21) (a) Bernardi, F.; De, S.; Olivucci, M.; Robb, M. A. *J. Am. Chem. Soc.* **1990**, *112*, 1737. (b) Palmer, I. J.; Ragazos, I. N.; Bernardi, F.; Olivucci, M.; Robb, M. A. *J. Am. Chem. Soc.* **1993**, *115*, 673−682. (c) Olivucci, M.; Ragazos, I. N.; Bernardi, F.; Robb, M. A. *J. Am. Chem. Soc.* **1993**, *115*, 3710−3721. (d) Olivucci, M.; Bernardi, F.; Celani, P.; Ragazos, I. N.; Robb, M. A. *J. Am. Chem. Soc.* **1994**, *116*, 1077−1085. (e) Celani, P.; Ottani, S.; Olivucci, M.; Bernardi, F.; Robb, M. A. *J. Am. Chem. Soc.* **1994**, *116*, 10141−10151. (f) Yamamoto, N.; Bernardi, F.; Bottoni, A.; Olivucci, M.; Robb, M. A.; Wilsey, S. *J. Am. Chem. Soc.* **1994**, *116*, 2064. (g) Bearpark, M. J.; Olivucci, M.; Wilsey, S.; Bernardi, F.; Robb, M. A. *J. Am. Chem. Soc.* **1995**, *117*, 6944−6953. (h) Bernardi, F.; Olivucci, M.; Robb M. A. *Isr. J. Chem.* **1993**, *33*, 265−276. (i) For a recent introduction see: Michl, J.; Klessinger, M. *Excited States and Photochemistry of Organic Molecules*; VCH: New York, 1995.

(22) (a) Bernardi, F.; Olivucci, M.; Robb, M. A. *J. Am. Chem. Soc.* **1992**, *114*, 1606−1616. (b) Bearpark, M. J.; Bernardi, F.; Olivucci, M.; Robb, M. A. *Chem. Phys. Lett.* **1994**, *217*, 513−519.

(23) Helgaker, T.; Uggerud, E.; Jensen, H. J. Aa. *Chem. Phys. Lett.* **1990**, *173*, 145−150.

(24) Chen, W.; Hase, W. L.; Schlegel, H. B. *Chem. Phys. Lett.* **1994**, *228*, 436−442.

(25) (a) Preston, R. K.; Tully, J. C. *J. Chem. Phys.* **1971**, *54*, 4297. (b) Preston, R. K.; Tully, J. C. *J. Chem. Phys.* **1971**, *55*, 562.

(26) Bearpark, M. J.; Bernardi, F.; Olivucci, M.; Robb, M. A. *Int. J. Quantum Chem.* In press.

(27) McWeeney, R.; Sutcliffe, B. T. *Molecular Quantum Mechanics;* Academic Press: New York, 1969; pp 148−170.

(28) Sklar, A. L. *J. Chem. Phys.* **1937**, *5*, 669.

Table 1. CASSCF/4-31G and MMVB Energies at Optimized Geometries for the S_0, S_1, and S_2 Planar Fulvene Structures, Together with the Planar and Twisted S_0/S_1 Intersections (Optimized CASSCF and MMVB Geometries Are Shown in Figures 2 and 3)

geometry	figure no., structure	ΔE(4-31G)/ kcal mol^{-1}	E(MMVB)/ kcal mol^{-1}	state
S_0 planar	2, **a**	0.0	0.0	S_0
		97.8 (79.3)^a	126.7	S_1
		142.0 (121.6)^a	148.6	S_2
S_1 planar^b	2, **b**	34.1	51.2	S_0
		62.3 (56.3)^{a,c}	67.9	S_1
S_2 planar	2, **c**	24.2	28.2	S_0
		75.9	88.9	S_1
		114.6 (107.9)^a	110.7	S_2
S_0/S_1 planar^d	3, **d**	65.9^e	69.5	S_0
		68.9^e	69.6	S_1
S_0/S_1 twisted	3, **e**	61.6^e	61.3	S_0
		61.7^e	61.3	S_1

[a] Experimental results from ref 7 in parentheses. [b] Second-order saddle point at CASSCF/4-31G. [c] Pyramidal minimum ~30 cm^{-1} lower in energy. [d] Unstable with respect to methylene twisting. [e] State-averaged orbitals.

Table 2. CASSCF/6-31G* Energies at Reoptimized Geometries and CASMP2/6-31G* Energies for the S_0 and S_1 Minima and the Planar and Twisted S_0/S_1 Surface Crossings

geometry	structure	ΔE(6-31G*)/kcal mol^{-1}	ΔE(MP2)	state
S_0 planar	**a**	0.0	0.0	S_0
		97.1	96.4	S_1
		142.3	145.5	S_2
S_1 planar^a	**b**	34.2	35.6	S_0
		61.4	62.8	S_1
S_0/S_1 planar^b	**d**	70.1		S_0
		70.3	72.2	S_1
S_0/S_1 twisted	**e**	58.2		S_0
		59.8	60.4	S_1

[a] Second-order saddle point at CASSCF/4-31G. Frequencies not recomputed. [b] Unstable with respect to methylene twisting.

by ~20 kcal mol^{-1}, and that MMVB further overestimates the CASSCF S_1 value by another 25 kcal mol^{-1}. Using the same active space and a DZ basis set, Dreyer and Klessinger[5] report CASSCF errors of the same magnitude.[29] Table 2 shows that adding one shell of polarization functions (6-31G*) leads to little improvement, and that the MP2 correction to the CAS6 energies is approximately the same for each state.

A ~20 kcal mol^{-1} error in the predicted excitation energies for covalent states is unusual in this type of system: typical errors in polyenes and aromatics[30] are ~5 kcal mol^{-1}. However, because the observed spectrum is weak, broad, and diffuse and the computed excitation energies are sensitive to small errors in the computed S_0 geometry, the 0−0 excitation energy is a better indicator of the quality of the potential energy surface. Table 1 shows that, at the CASSCF and MMVB levels of theory, we reproduce the S_1 and S_2 experimental 0−0 transition energies to within few kilocalories per mole using structures **b** and **c** as the corresponding excited state structures.

(2) The S_1 Potential Energy Surface and S_0/S_1 Conical Intersection. Considering only planar C_{2v} geometry changes first, the S_0 and S_1 potential energy surfaces of fulvene and azulene[3] have the same topology. A cut along the C_{2v} $S_0^* \rightarrow S_1$ coordinate (which bisects the surfaces illustrated in Figure 1) is presented in Scheme 2: Steep relaxation on S_1 in fulvene leads to a flat region of the potential in which S_0 and S_1 are approximately 20 kcal mol^{-1} apart. Continuing along the $S_0^* \rightarrow S_1$ coordinate through the planar minimum **b** leads to a sloped[2q] S_0/S_1 surface crossing at a very similar geometry (**d** in Figure 3) where decay to the ground state can be fully efficient. As with azulene, there is no intervening transition structure along the C_{2v} relaxation path, and the momentum developed from S_0^* (35 kcal mol^{-1} calculated, ~20 kcal mol^{-1} experimental) will be more than sufficient to reach the S_0/S_1 crossing point (which is only 9 kcal mol^{-1} above the minimum in fulvene).

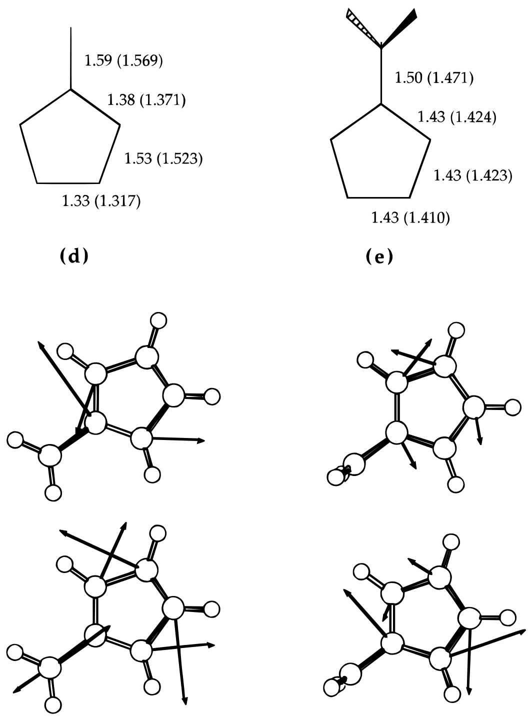

Figure 3. The planar **d** and twisted **e** critical points on the S_0/S_1 intersection—MMVB bond lengths (Å) (CASSCF/4-31G values in parentheses). The corresponding derivative coupling (middle) and gradient difference (bottom) vectors—directions which lift the degeneracy at each point—are also shown.

Scheme 2

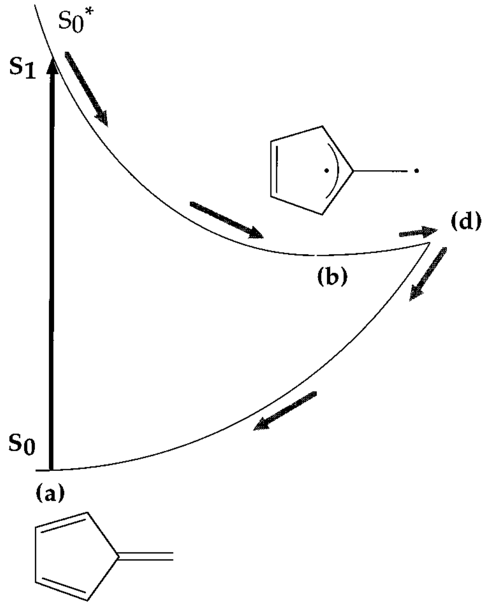

The S_0 and S_2 planar structures **a** and **c** in Figure 2 are found to be true energy minima at both CASSCF and MMVB levels of theory. However, the planar structure **b** optimized on S_1 with CASSCF is found to be a local maximum with one shallow

---

(29) Negri and Zgierski (CASSCF/3-21G, ref 6) report an S_1 vertical excitation energy of 3.644 eV/84 kcal mol^{-1}—an error of only 5 kcal mol^{-1}. We calculate 100.7 kcal mol^{-1} in the same basis.

(30) (a) Roos, B. O.; Andersson, K.; Fulscher, M. P. *Chem. Phys. Lett.* **1992**, *192*, 5−13. (b) Serrano-Andres, L.; Merchan, M.; Nebotgil, I.; Lindh, R.; Roos, B. O. *J. Chem. Phys.* **1993**, *98*, 3151−3162.

Table 3. CASSCF/6-31+G* Relative Energies (kcal mol^{-1}) at the RHF/STO-3G Twisted Ionic Geometry **h** Shown in Figure 4, using 6-, 7-,[a] and 9-Orbital[a] Active Spaces

	CAS(6,6)	CAS(6,7)	CAS(6,9)	dipole/D
$\Delta E(S_0/S_1 \rightarrow S_2)$	60.6	57.6	53.7	<0.1
	(39.6)	(39.8)		7.7[c]

[a] π-orbitals with extra nodes above and below the ring added to the active space. [b] CASMP2/6-31+G* values in parentheses. The use of the RHF/STO-3G geometry is discussed in the Computational Details section. [c] Negative charge on the ring.

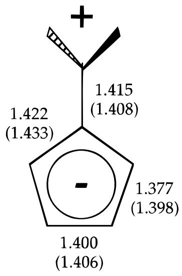

(h)

Figure 4. RHF/STO-3G twisted ionic geometry **h**. Bond lengths in Å. Negative charge on the ring. (Reoptimized bond lengths at the CASSCF/6-31+G* level are shown in parentheses).

negative direction of curvature (278i cm^{-1}) corresponding to methylene twisting, and another (307i cm^{-1}) leading to a slightly-pyramidal structure ~30 cm^{-1} lower in energy.[5,6] (The MMVB surface in this region is essentially flat along the twisting coordinate). Following the 278i cm^{-1} mode leads ultimately to a 90° twisted structure (**e** in Figure 3) which is ~2 kcal mol^{-1} lower than **b** in energy (Tables 1 and 2) and is the lowest-energy point on S_1. Here, the methylene group p-orbital is perfectly decoupled from the ring, which is approximately 5-fold symmetric with C−C bond lengths of 1.43 Å. The gradient of the energy on S_1 does not go to zero at this point because it is a point of intersection. Thus, structure **e** corresponds to a peaked[2q] S_0/S_1 crossing structure very similar to the one previously located by Klessinger.[5]

The planar S_0/S_1 crossing (**d** in Figure 3) like the S_1 planar structure (**b** in Figure 2) is unstable with respect to methylene twisting. Figure 3 shows that the gradient difference and derivative coupling vectors computed at both crossing points **d** and **e**—the directions which lift the degeneracy[19]—do not involve the methylene twist, which means that the crossing must exist for all twist angles (Figure 1). However, the actual twist angle at which S_1 fulvene decays on relaxation from S_0^* will depend on the details of the nuclear dynamics, which will be discussed below in subsection 4.

(3) Origin of the Crossing. A critically-symmetric biradicaloid S_0/S_1 crossing is often postulated for double bond isomerization.[2k−m,16] Table 3 shows that the ring$^-$ methylene$^+$ ionic state is S_2 at the RHF/STO-3G twisted geometry (**h** in Figure 4), about 60 kcal mol^{-1} above the degenerate S_0 and S_1 states. Reoptimising at the 6-orbital CAS/6-31+G* level lowers the S_2 energy by only 5 kcal mol^{-1} (Figure 4 and Table 3). Both an enlarged active space and the MP2 correction lower the S_2 energy further, but not by so much that an ionic/covalent crossing in this region is likely. Conditions for a critically-symmetric biradicaloid S_0/S_1 crossing do not therefore appear to be fulfilled in this case.

Scheme 3

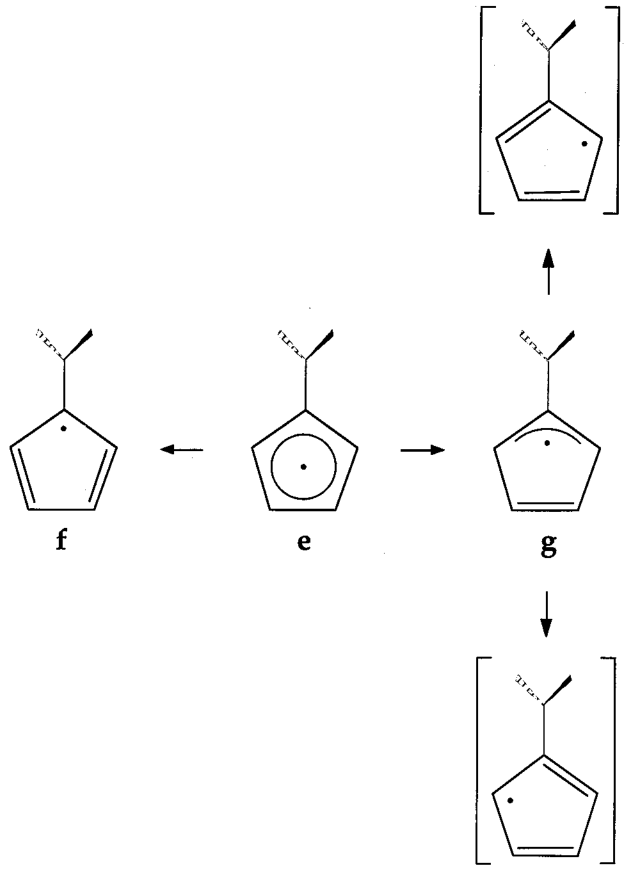

Table 4. CASSCF/4-31G Energies (relative to **a**) for the Twisted Transition Structures on the Fulvene S_0 Surface (Optimized Geometries and the Corresponding Transition Vectors Are Shown in Figure 6

geometry	figure no.	ΔE(4-31G)/ kcal mol^{-1}	ΔE(MMVB)/ kcal mol^{-1}	state
adiabatic S_0	6f	54.6	53.9	S_0
isomerization		76.1	83.2	S_1
S_1-like	6g	56.5	53.9	S_0
ring recoupling		74.1	82.9	S_1

Because the methylene group and ring π-systems are decoupled at **e** (Figure 3) the S_0/S_1 crossing in fulvene is analogous to the the Jahn−Teller degeneracy of the D_0 and D_1 states of the cyclopentadienyl radical.[31] In cyclopentadienyl, there are two coordinates which lift the degeneracy:[32] one leading to a minimum having two localized double bonds and an unpaired electron, the other leading to a transition structure a few cm^{-1} higher in energy with an allyl group and a single double bond.[33] Scheme 3 and Figure 5 show how these distortions in fulvene lead to critical points on S_0 in the vicinity of the twisted conical intersection **e**. The cyclopentadienyl D_0 minimum correlates with the twisted fulvene structure **f** (Figure 6). However, **f** is not a fulvene minimum but a transition structure for adiabatic isomerization on S_0, which lies ~55 kcal mol^{-1} above the ground state minimum **a** (Tables 1 and 4). The cyclopentadienyl D_0 transition structure correlates with the fulvene twisted transition structure **g** (Figure 6). In fulvene, however, the minima which this particular transition vector points toward (which are shown in Scheme 3 in square brackets) cannot be located: an IRC calculation leads to a region of S_0 in which the methylene starts to become planar and the gradient is steep.

---

[31] (a) Yu, L.; Foster, S. C.; Williamson, J. M.; Heaven, M. C.; Miller, T. A. *J. Phys. Chem.* **1988**, *92*, 4263−4266. (b) Yu, L.; Williamson, J. M.; Miller, T. A. *Chem. Phys. Lett.* **1989**, *162*, 431−436. (c) Yu, L.; Cullin, D. W.; Williamson, J. M.; Miller, T. A. *J. Chem. Phys.* **1993**, *98*, 2682−2698. (d) Borden, W. T.; Davidson, E. R. *J. Am. Chem. Soc.* **1979**, *101*, 3771−3775.

[32] Reference 2f, pp 48−51.

[33] Bearpark, M. J.; Robb, M. A.; Yamamoto, N.; Olivucci, M.; Bernardi, F. In preparation.

Table 5. MMVB Dynamics Data: Initial and Hop Energies Are Measured with Respect to the S_1 Planar Structure **b** (Figure 2)

$\Delta E_{\text{limit}}/E_h$	initial S_1 energy/ kcal mol^{-1}	hop S_1 energy/ kcal mol^{-1}	ΔE at hop/ kcal mol^{-1}	KE at hop/E_h	hop time/fs	total time/fs	% hop $S_1 \rightarrow S_0$	initial methylene torsion angle/deg
0.0001	0.3 ± 0.05	−1.1 ± 0.2	1.9 ± 0.6	$(1.8 \pm 0.2) \times 10^{-3}$	156 ± 46	304 ± 89	27	180 ± 11
0.001	2.5 ± 0.6	0.4 ± 0.7	2.9 ± 0.9	$(3 \pm 1) \times 10^{-3}$	36 ± 27	79 ± 36	57	180 ± 19
0.004	12 ± 3	6 ± 3	4 ± 1	$(9 \pm 4) \times 10^{-3}$	16 ± 13	45 ± 15	54	180 ± 26
0.008	24 ± 6	14 ± 6	5 ± 2	$(16 \pm 8) \times 10^{-3}$	12 ± 12	30 ± 10	73	180 ± 27

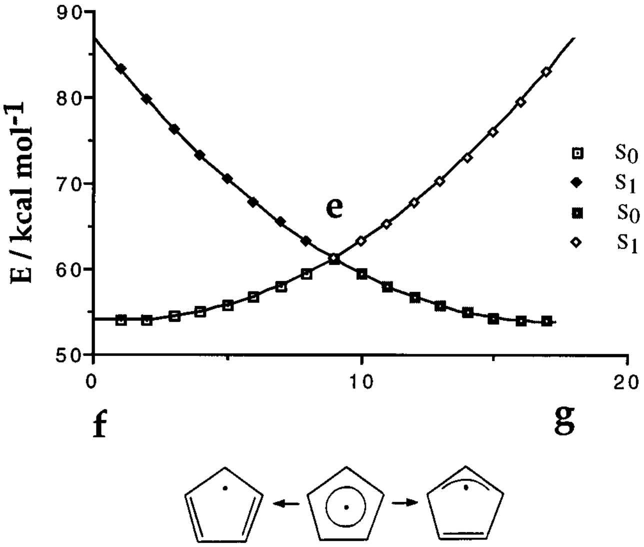

Figure 5. An MMVB linear interpolation between the adiabatic isomerization **f** and S_1-like **g** twisted transition structures on S_0 and the twisted crossing **e**. Structures **e**−**g** are shown in Figures 3 and 6. Energies are relative to the planar S_0 minimum **a** in Figure 2.

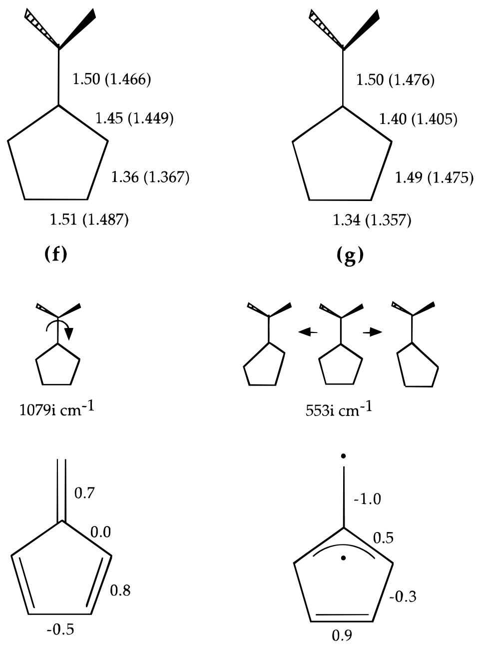

Figure 6. Twisted transition structures and associated vectors on S_0. Left: Adiabatic methylene isomerization. Right: S_1-like ring recoupling. MMVB bond lengths in Å (CASSCF/4-31G values in parentheses). The corresponding S_0 P_{ij} (π electron exchange density) values are shown at the bottom.

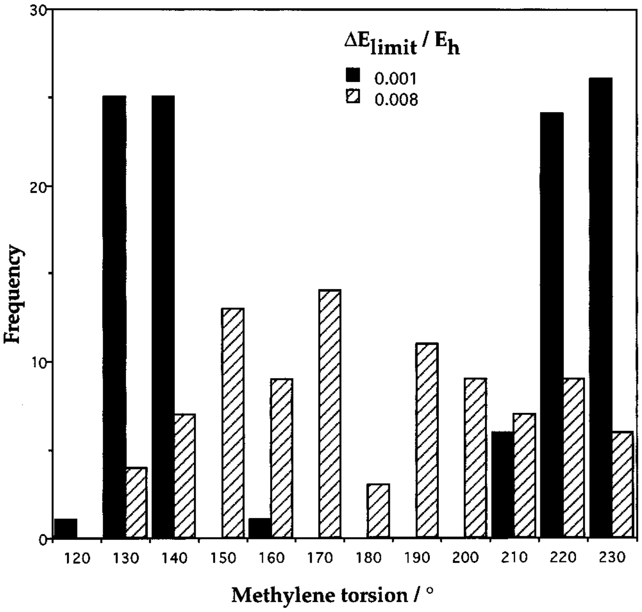

Figure 7. MMVB dynamics. Methylene torsion angle (defined in Scheme 1) in degrees at the hop geometry as a function of initial excess energy ΔE_{limit}. The frequency is defined as the number of trajectories which hopped with a particular range of methylene torsion angles out of a total of 128.

The P_{ij} matrices for **f** and **g** (Figure 6, bottom) show that **f** is on the S_0-like branch of the crossing, whereas **g** correlates diabatically with S_1.

(4) Dynamics Simulation. Our objective is to model the excited state dynamics following 0−0 excitation (because of the uncertainty in the vertical excitation energies). Although MMVB reproduces the CASSCF S_1 surface topology, there are still differences in the energetics: (i) The CASSCF twisted conical intersection structure **e** lies 8 kcal mol^{-1} below the planar conical intersection structure **d**, but this difference is 12 kcal mol^{-1} with MMVB. (ii) The energy difference **b** → **d** (S_1 minimum → S_1/S_0 conical intersection) is 10 kcal mol^{-1} with CASSCF but only 1.5 kcal mol^{-1} with MMVB.

Disagreement between *ab initio* and MMVB energy differences is associated with a simple structural effect: MMVB overestimates the $C_5H_4{-}CH_2$ bond length at the S_1 minimum **b** by 0.05 Å, and hence the increase in this bond length on going **b** → **d** is only 0.04 Å at the MMVB level but 0.08 Å with CASSCF. This results in both a smaller **b** → **d** energy difference and a larger **b** → **e** energy difference with MMVB. In our dynamics computations, the surface hop does not generally occur at the minimum in the $n - 2$ dimensional intersection space, but rather at higher energy points, and we assume that these limited structural changes will not affect the general conclusions of the simulation.

MMVB dynamics results are collected in Table 5. Four values of the mode-sampling threshold ΔE_{limit} have been used, leading to initial vibrational energy distributions from 0.3 ± 0.05 to 24 ± 6 kcal mol^{-1}. Because the MMVB S_1 potential is essentially flat along the methylene twist coordinate in the region of **b**, twisting will be the major geometric change when ΔE_{limit} is small. For $\Delta E_{\text{limit}} = 0.001E_h$, the initial twist angle (measured as the dihedral shown in Scheme 1) is 180 ± 19°. In Figure 7 we show that this angle has relaxed at the hop to either 130−140° or 220−230°, suggesting that a twisted region of the $n - 2$ dimensional crossing has been reached in ~36 fs (Table 5). However, as the initial excess energy at **b** is increased ($\Delta E_{\text{limit}} = 0.008E_h$, Figure 7) we find that the hop is most likely to take place at almost planar geometries (180 ± 50°) in a fraction of the time (∼12 fs). In this case, the spread of the initial wavepacket is larger and more of the intersection space consequently becomes accessible, including the higher-energy planar region of the crossing. Furthermore, the increased kinetic energy can now overcome a larger hop gap in this semiclassical model,[34] enlarging the space at which a surface hop may occur.

None of the trajectories in our simulation resulted in isomerisation. After decay at the 90° twisted S_0/S_1 crossing minimum, which can be reached only at zero KE, relaxation to the planar S_0 geometry can occur in either direction with equal probability. However, at higher-energy points on the crossing—at twist angles away from 90°—the steep gradient on S_0 actually favors relaxation back to the original planar structure.

Conclusion

We have found that the fulvene S_0/S_1 crossing minimum—the lowest-energy-point on S_1—corresponds to the 90° twisted geometry described by Klessinger.[5] The existence of such an accessible conical intersection between the S_0 and S_1 states of fulvene explains the lack of observed fluorescence, leading to efficient and irreversible decay.

Semiclassical dynamics calculations with MMVB (and energies computed at CASMP2/6-31G*) suggest that, for vibrationally excited S_1 fulvene, $S_1 \rightarrow S_0$ decay is actually more likely to occur in the planar azulene-like crossing region which is located some 12 kcal mol^{-1} higher in energy than the twisted crossing minimum but ∼30 kcal mol^{-1} lower than the vertically excited geometry S_0^*. As with azulene[3] the $S_1 \rightarrow S_0$ decay takes place in femtoseconds before a single oscillation through the crossing line is completed. Because of this (and the fact that the gradient for twisting is so steep on S_0) we predict that isomerization of the exocyclic methylene may only be detected after 0−0 excitation to S_1.[35]

Acknowledgment. This research has been supported in part by the SERC (UK) under Grant Nos. GR/J25123 and GR/H58070. All *ab initio* computations were run on an IBM RS/6000 using a development version of the Gaussian 94 program.[17] MMVB computations were run on a Cray T3D at the Parallel Computing Centre, University of Edinburgh (EPCC).

Supporting Information Available: Tables 1a−4a giving CASSCF energies in hartrees (4 pages). Ordering information is given on any current masthead page.

JA9542799

---

[34] Reference 2j, pp 153−156

[35] As far as we are aware, isomerization of suitably-labeled fulvene derivatives has not yet been studied.